PERGAMON

Building and Environment 36 (2001) 407–419

BUILDING AND ENVIRONMENT

www.elsevier.com/locate/buildenv

Three-dimensional analysis of thermal resistance of exterior basement insulation systems (EIBS)

W. Maref*, M.C. Swinton, M.K. Kumaran, M.T. Bomberg

National Research Council of Canada, Institute of Research in Construction, M-24 Montreal Road, Ottawa, Canada K1A 0R6

Received 20 July 1999; received in revised form 18 October 1999; accepted 8 February 2000

Abstract

A consortium[1] research project was initiated to determine the field performance of various thermal insulation products as applied in the exterior insulation basement system (EIBS). Initially a two-dimensional (2-D) analytical tool was used to derive the thermal transmission characteristics from an array of temperature measurements performed over a period of two years. Results immediately showed the influence of lateral heat flux between various products that differed in thermal transmission properties. Therefore, development of a three-dimensional (3-D) model became imperative.

This paper gives the theoretical and numerical approaches adopted to develop a 3-D computer model of heat transfer. The implicit Spline Method was selected for the problem solver. The applicability of the model was verified using measured data on temperature distributions at several material interfaces. Then the model was used to estimate the effect of lateral heat flows.

The paper also briefly reports the experimental details and presents results on model verification.

Keywords: Exterior insulation; Thermal resistance; Thermal performance; Heat transfer; Basement walls; Three-dimensional (3-D) model; Calculation; Analysis; Temperature; Heat flow; Heat loss

1. Background

Over recent decades, a large part of basements in newly built Canadian houses became used as a habitable space. This, combined with increased requirements for energy conservation, resulted in the development of many insulated basement systems. While thermal insulation may be placed either on the inside or outside of the basement wall, the material choice and the insulation placement may affect overall performance of the basement wall. Some external insulation systems, in addition to controlling heat losses, may also increase durability of the basement wall.

In this context, the Canadian thermal insulation industry, working together with the National Research Council, decided to revisit[2] the design and performance of external insulation basement systems (EIBS). Over the two-year period from June 1996 to June 1998, 10 expanded polystyrene (EPS), two spray polyurethane foam (SPF), two mineral fibre insulation (MFI) and two glass fibre insulation (GFI) specimens were placed on the exterior of the basement wall in an experimental building located on the NRC Campus in Ottawa.

This research project involved a number of material and system issues. Material considerations involved the selection of existing and new thermal insulation products (being under development). These products were placed side-by-side on the basement wall to create virtual test compartments. The system considerations

* Corresponding author. Tel.: +1-613-993-5709; fax: +1-613-954-3733.

E-mail address: wahid.maref@nrc.ca (W. Maref).

[1] The consortium included the Expanded Polystyrene Association of Canada, the Canadian Urethane Foam Contractors Association, Owens Corning Inc. and Roxul Inc.

[2] See previous publications: Tao et al. [1], Bomberg [2].

0360-1323/00/$ - see front matter
PII: S0360-1323(00)00022-6

Nomenclature

C	specific heat [J/kg K]
K_i	thermal conductivity in the x-direction [W/m K]
K_j	thermal conductivity in the y-direction [W/m K]
K_k	thermal conductivity in the z-direction [W/m K]
Q	heat generation [W/m^3]
S_1, S_2, S_3	boundary surfaces
t	time [s]
T_0	initial temperature [°C]

Greek symbols

Δt	time step [s]
Δx, Δy, Δz	step of spatial discretisation in the x-, and z-directions [m]
ρ	density [kg/m^3]

Subscripts

i	nodal point value
j	nodal point value
k	nodal point value
s	on boundary surface

involved two different technical solutions to protect the above-grade part of the EIBS. Furthermore, different conditions for surface water drainage were implemented on east and west walls of the NRC experimental basement facility.

Because of the wide scope of the basement research, this project is reported in four parts:

1. Development of analytical tools to increase confidence in the experimental results and facilitate the analysis of the field data.
2. Reporting and analysing results obtained from the experimental basement.
3. Placing the thermal and moisture performance of EPS in below-grade application in context of other research (state-of-the-art review to identity future research needs on the material side).
4. Reporting and analysing the system effects in context of other research (state-of-the-art review to identity future research needs for development of basement systems).

The first part of the EIBS project is addressed in this paper, which presents theoretical and numerical aspects of a 3-D computer model developed as part of an integrated approach (modelling and testing). The capabilities of this model to enhance the analysis of experimental results will be demonstrated in the next paper [3].

2. Experimental approach

To evaluate the performance of exterior basement insulation, different materials were installed on the exterior surface of concrete basement walls. As shown in Fig. 1, eight test specimens were placed side-by-side, on each of two basement walls (east and west) insulating a whole wall with approximately 76-mm thick and 2.4 m high specimens. On the interior of the wall, a 25-mm layer of EPS board was installed over entire surface. At three vertical locations on each wall, cut-outs were made and calibrated EPS sp mens, with identical thickness, were tightly inser These specimens were used for the determination transient heat flux entering the wall [4].

Thermocouples were placed at the boundary s faces, as well as the interfaces of each layer in the w in an array consisting of 16 points per tested comp. ment. All sensors placed on the west wall are show Fig. 2.

The parameters monitored in the EIBS are:

1. Surface temperatures, on both sides of the c brated specimen, the concrete and the test sp mens.
2. Heat flux across the calibrated insulation specime
3. Soil temperatures from 1 to 2 m away from the s cimens, and at five depths.
4. Interior basement air temperature (an average four readings).
5. Exterior air temperature (at the north face, shield from the Sun).
6. Relative humidity (RH) and other parameters indoor and outdoor environments.

The instrumentation package consisted of appro mately 145 thermocouples, two humidity sensors, calibrated insulation specimens (heat flux transducer four junction boxes, and a data acquisition unit op ated by a computer.

2.1. Data acquisition

The collection of data was done with an automat data acquisition and scanning system, and a high pr cision multi-meter to measure separate thermocouple serial thermopiles and RH sensors. All thermocoupl and power signals were routed through an HP co mand module (HP E1406) connected to a PC 486/5

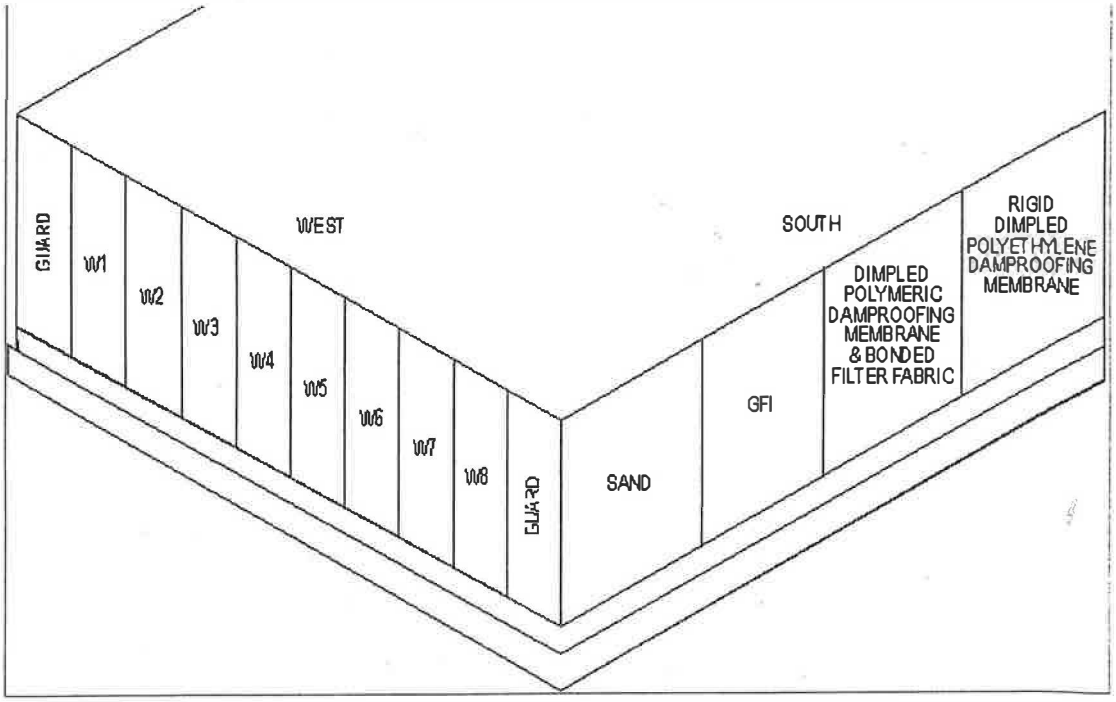

Fig. 1. Schematic of placement of specimens on the west wall.

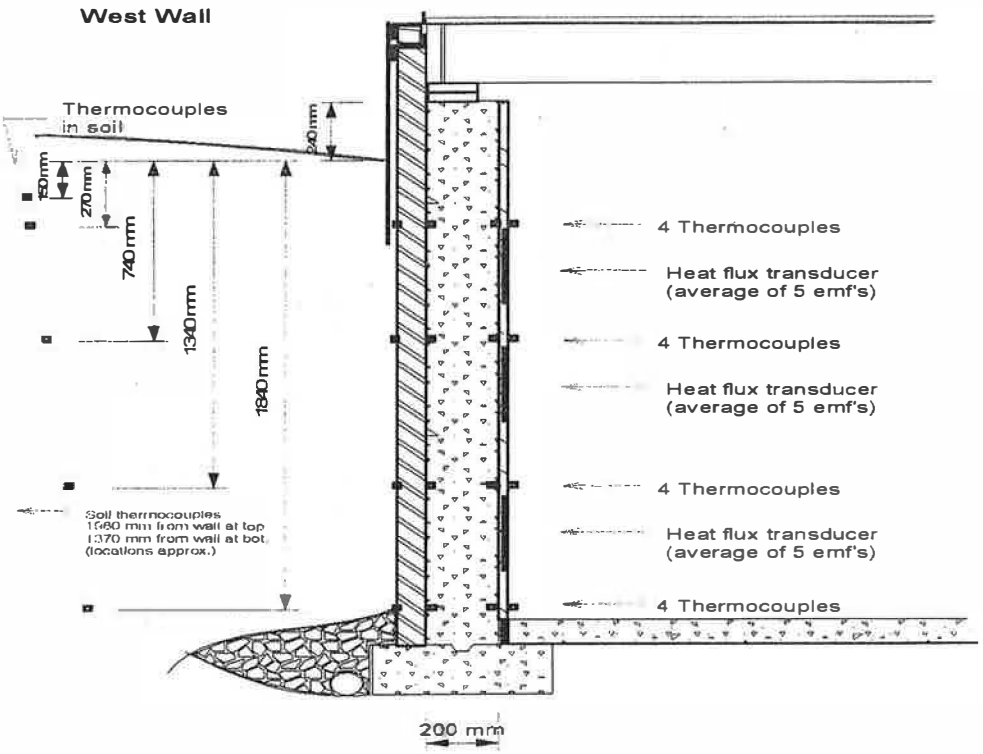

Fig. 2. Thermocouples and calibrated insulation specimens mounted on the west wall.

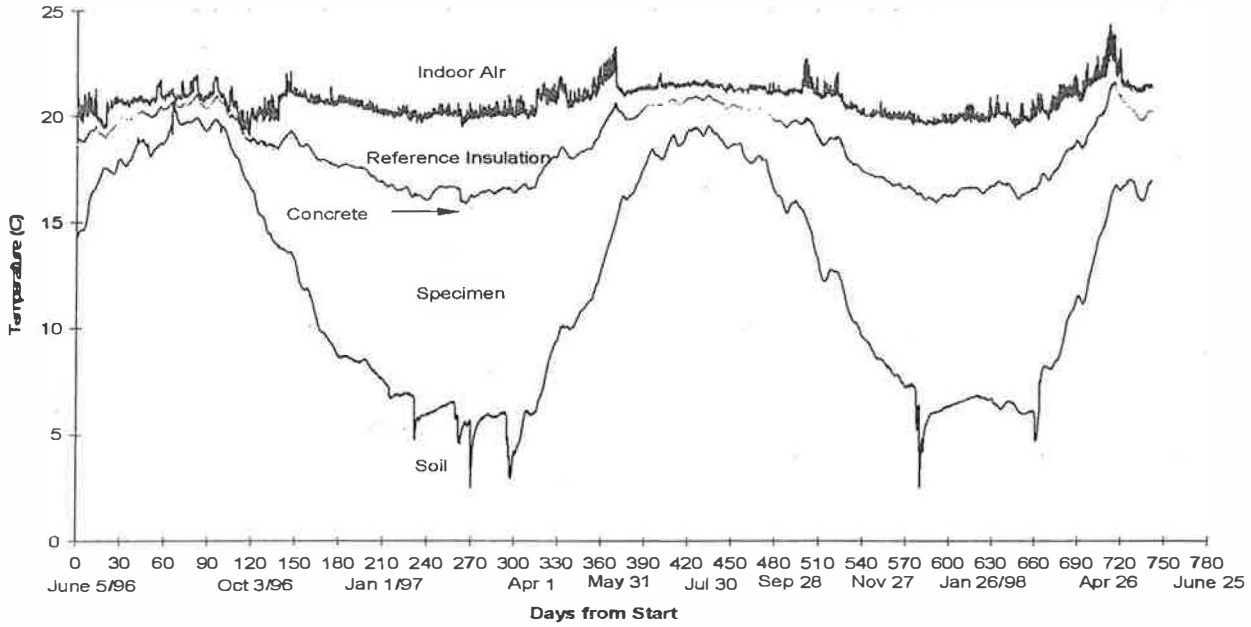

Fig. 3. Temperatures across the W6 specimen measured in the mid-height position.

Measurements were taken every 2 min and averaged by the software package (HP_VEE) for 10-min intervals for the wall thermocouples (five readings), and 30-min intervals for the soil thermocouples (15 readings).

2.2. Duration of the experimental program

The data acquisition system was commissioned in the spring of 1996 and monitoring started after adjusting the air conditioning system on 5 June 1996. The monitoring ended on 5 June 1998, exactly two full years of monitoring.

Fig. 3 shows the measured temperatures of indoor air, calibrated insulation specimens, concrete, and soil surface in the "mid-position" of the wall over a period of two years. The spikes in the interface between the soil and the EIBS correspond to the thaw periods with a heavy rainfall. Observe that these effects do not appear to affect the temperature on the concrete surface, i.e., behind the external insulation.

Fig. 4 shows the special treatment at the interface.

2.3. Preliminary results

Examination of the preliminary results highlighted the difficulties in establishing the precision of thermal testing without addressing 3-D effects. This is best illustrated by comparing W5 and W6 tested wall sections.

Table 1a shows the average temperature difference across the insulation layer and heat fluxes entering each of these two tested wall sections. These results are averaged over a period of one week to approximate the steady state and use the ratio between the temp ture difference and the heat flux as an indicator thermal resistance. When thermal resistance of W taken as a benchmark (100%), the ratio between and W5 specimens is 122%. This result is, howe much lower than the ratio of 164% obtained from initial laboratory measurements of thermal resista performed on specimens W5 and W6. Even if the value of the W6 specimen was corrected for the ef of foam ageing, the difference between the one-dim sional (1-D) estimate and the measured results is nificant. This difference highlights the need for a model application.

2.4. Discussion

As the test set-up involved diverse thermal insulat materials placed next to each other, the presence lateral heat flow was inevitable. In the case of spe men W6 (closed-cell, gas-filled thermal insulat foam), some heat would be conducted latera through the concrete wall and pass through the ad cent specimen, which has a lower thermal resistan The lateral heat flow may explain that the ratio of e mated thermal resistance of two adjacent specim W5 and W6 (shown in Table 1b) is smaller than ratio indicated by the laboratory comparison.

To evaluate the effects of lateral heat flow on precision of the field measurements, a new task w added to the EIBS project, namely, the developme of a 3-D model. The first question was then, how discretise the continuous equations to arrive at the s tem, which is easy to solve with numerical technique

Table 1a
Measured temperature, heat flux and temperature difference across the insulation specimen, averaged over the week 9–16 December 1996

Position	Specimen			
	W5		W6	
	Temperature inside specimen (°C)	Temperature outside specimen (°C)	Temperature inside specimen (°C)	Temperature outside specimen (°C)
Bottom	16.91	14.37	16.78	13.55
Low	17.38	12.30	17.44	11.67
Middle	16.82	9.60	17.14	8.49
High	15.98	5.24	16.47	4.37
Average temperature	16.77	10.38	16.96	9.52

3. Solution of the differential equation of heat conduction

3.1. State-of-the-art of analytical techniques

Several different techniques of numerical analysis for solving transient heat conduction problems, such as the finite-difference, finite-element, and boundary integral equation methods have been presented in the technical literature.

Bhattacharya [5] and Lick [6] applied the improved finite-difference method (FDM) to time-dependent heat conduction problems with step-by-step computation in the time domain. The finite-element method (FEM) based on a variational principle, was used by Gurtin [7] to analyse the unsteady problem of heat transfer. Emery and Carson [8], as well as Visser [9], applied variational formulations in their finite-element solutions of non-stationary temperature distribution problems. Bruch and Zyvolovski [10] solved the transient linear and non-linear 2-D heat conduction problems using the finite-element weighted residual process. Rources and Alarcon [11] presented a formulation for a 2-D isotropic continuous solid using the boundary integral equation method (BIEM) with a finite-difference approach in the time domain. Combined application of BIEM and the Laplace transform to transient heat conduction problems started in 1970 with a paper by Rizzo and Shippy [12]. Later, Liggett and Liu [13] and Cheng and Liggett [14] applied this scheme to the linear time-dependent problems. Chen et al. [15] successfully applied a hybrid method based on the Laplace transform and the FDM to transient heat conduction problems.

The disadvantages of these methods are: complicated procedure; need for large storage; and long computation time. Wang et al. [16] used the implicit spline method of splitting to solve the 2- and 3-D transient heat conduction problems. The method is applied to homogeneous and isotropic solids.

A cubic spline method has been developed in the numerical integration of partial differential equations since the pioneering work of Rubin and Graves [17], and Rubin and Khosla [18]. This method provides a simple procedure, small storage, short computation time, and a high order of accuracy. Furthermore, the spline method has a direct representation of the gradient boundary condition.

In this paper, an implicit spline method is used for the solution of 3-D transient heat conduction problems for a non-homogeneous medium. This method, for each computation step, treats the problem as a 1-D case in the implicit form and only one tri-diagonal system is evaluated. In Section 2, a spline scheme of splitting is presented. In Section 3, the stability of the method is assessed.

Table 1b
Apparent steady-state thermal resistance of specimens W5 and W6 calculated from data shown in Table 1a

	W5	W6
Temperature difference across the wall, K	6.39	7.44
Mean heat flux on inner surface, W/m^2	4.30	4.10
Apparent R-value, (m^2 K)/W	1.49 (100%)	1.81 (122%)

3.2. Mathematical formulation

The governing differential equation for transient heat conduction in a homogeneous and isotropic solid is given by:

$$\rho C\frac{\partial T}{\partial t} = \left(\frac{\partial}{\partial x}\left(K_i\frac{\partial T}{\partial x}\right) + \frac{\partial}{\partial y}\left(K_j\frac{\partial T}{\partial y}\right) + \frac{\partial}{\partial z}\left(K_k\frac{\partial T}{\partial z}\right)\right) + Q \tag{3.1}$$

This equation, with suitable boundary and initial conditions, represents the problem of temperature distribution at any time and at any point of the volume under consideration.

Different density ρ, but constants for each type were used. They were determined as the average of several specimens. Discussion on EPS variability in physical properties and the method that has been used for their homogenisation is currently published [19].

The specific heat C which appears in Eq. (3.1) and consistently further was from the Handbook of Heat Transfer.

The above quoted paper [19] deals with the thermal conductivity coefficient as it varies with material thickness, temperature, density of the specimen and the specific mass extinction coefficient. As far as Q is concerned, it is a result of gradient T and K.

Thermal conductivity K_i in Eq. (3.1) does not include any effect of latent heat transfer that may be induced by the humidity changes.

3.2.1. Special treatment at the interface

Assuming the perfect contact, i.e., when heat fluxes ϕ_{ic} and ϕ_{ici} are equal, the following equation is obtained:

$$K_{i+1/2} = \frac{K_i K_{i+1}(X_{i,c} + X_{c,i+1})}{K_i X_{c,i+1} + K_{i+1} X_{i,c}}$$

and the interface temperature (Fig. 4) is given by:

$$T_c = \frac{K_i X_{c,i+1} T_i + K_{i+1} X_{i,c} T_{i+1}}{K_i X_{c,i+1} + K_{i+1} X_{i,c}}$$

3.2.2. Boundary and initial conditions

The temperatures are imposed at the surfaces:

$T = T_{S_1}$ on surface S_1

$T = T_{S_2}$ on surface S_2

$T = T_{S_3}$ on surface S_3

and the initial condition is:

$T(x, y, z, 0) = T_0(x, y, z)$

where the union of the surfaces S_1, S_2 and S_3 forms the complete boundary of the solid of volume S_2 and S_3 are part of the boundary on which tl peratures T are prescribed.

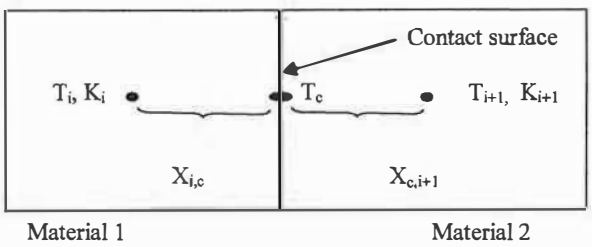

Fig. 4. Special treatment at the interface.

3.2.3. Implicit spline schemes

The implicit spline schemes of splitting for t merical solution of Eq. (3.1) are [20]:

$$T_{ijk}^{n+1/3} = T_{ijk}^{n} + \Delta \frac{1}{\rho C}\left(P_{ijk}^{n+1/3} + \frac{1}{3}Q\right)$$

$$T_{ijk}^{n+2/3} = T_{ijk}^{n+1/3} + \Delta t \frac{1}{\rho C}\left(R_{ijk}^{n+2/3} + \frac{1}{3}Q\right)$$

$$T_{ijk}^{n+1} = T_{ijk}^{n+2/3} + \Delta \frac{1}{\rho C}\left(S_{ijk}^{n+1} + \frac{1}{3}Q\right)$$

where T_{ijk}, P_{ijk}, R_{ijk} and S_{ijk} are the spline a mation of

$$(T)_{ijk}, \quad \left(\frac{\partial}{\partial x}\left(K_i \frac{\partial T}{\partial x}\right)\right)_{ijk}, \quad \left(\frac{\partial}{\partial y}\left(K_j \frac{\partial T}{\partial y}\right)\right)_{ijk},$$

$$\left(\frac{\partial}{\partial z}\left(K_k \frac{\partial T}{\partial z}\right)\right)_{ijk}$$

respectively, and there are spline relations as foll

$$\frac{\Delta x_{ijk}}{6} P_{i-1,jk} + \frac{(\Delta x_{ijk} + \Delta x_{i+1,jk})}{3} P_{i,jk} + \frac{\Delta x_{i+1,jk}}{6} P_{i+1,jk} = K_{i+1/2} \frac{(T_{i+1,jk} - T_{ijk})}{\Delta x_{i+1,jk}} - K_{i-1/2} \frac{(T_{ijk} - T_{i-1,jk})}{\Delta x_{i,jk}}$$

$$\frac{\Delta y_{ijk}}{6} R_{i,j-1,k} + \frac{(\Delta y_{ijk} + \Delta y_{i,j+1,k})}{3} R_{i,jk} + \frac{\Delta y_{1,j+1,k}}{6} R_{i,j+1,k} = K_{j+1/2} \frac{(T_{i,j+1,k} - T_{ijk})}{\Delta y_{i,j+1,k}} - K_{j-1/2} \frac{(T_{ijk} - T_{i,j-1,k})}{\Delta y_{i,jk}}$$

$$\frac{\Delta z_{ijk}}{6}S_{i,\,j,\,k-1}+\frac{(\Delta z_{ijk}+\Delta z_{ij,\,k+1})}{3}S_{i,\,jk}+\frac{\Delta z_{ij,\,k+1}}{6}S_{ij,\,k+1}=K_{k+1/2}\frac{(T_{ij,\,k+1}-T_{ijk})}{\Delta z_{ij,\,k+1}}-K_{k-1/2}\frac{(T_{ijk}-T_{ij,\,k-1})}{\Delta z_{i,\,jk}} \tag{3.3c}$$

where

$$\Delta x_{ijk}=x_{ijk}-x_{i-1,\,jk}>0$$

$$\Delta y_{ijk}=y_{ijk}-y_{i,\,j-1,\,k}>0$$

$$\Delta z_{ijk}=z_{ijk}-z_{ij,\,k-1}>0$$

If boundary conditions are given, we obtain spline solutions of Eq. (3.1) from Eqs. (3.2) and (3.3).

Eq (3.2a) can be written in the following form

$$T_{ijk}^{n+1/3}=E_{ijk}+F_{ijk}P_{ijk}^{n+1/3} \tag{3.4}$$

From Eqs. (3.2a) and (3.4), we find

$$A_iT_{i-1,\,jk}^{n+1/3}+B_iT_{ijk}^{n+1/3}+C_iT_{i+1,\,jk}^{n+1/3}=D_i,\quad i=2,N-1 \tag{3.5}$$

where

$$A_i=\frac{\Delta x_{ijk}}{6F_{i-1,\,jk}}-\frac{K_{i-1/2}}{\Delta x_{ijk}}$$

$$B_i=\frac{\Delta x_{ijk}+\Delta x_{i+1,\,jk}}{3F_{ijk}}+\frac{K_{i-1/2}}{\Delta x_{ijk}}+\frac{K_{i+1/2}}{\Delta x_{i+1,\,jk}}$$

$$C_i=\frac{\Delta x_{i+1,\,jk}}{6F_{i+1,\,jk}}-\frac{K_{i+1/2}}{\Delta x_{i+1,\,jk}}$$

$$D_i=\frac{\Delta x_{ijk}E_{i-1,\,jk}}{6F_{i-1,\,jk}}+\frac{(\Delta x_{ijk}+\Delta x_{i+1,\,jk})E_{ijk}}{3F_{ijk}}+\frac{\Delta x_{i+1,\,jk}E_{i+1,\,jk}}{6F_{i+1,\,jk}}$$

Under proper conditions this system can be solved with the Thomas Algorithm (A.D.I. Method) [21].

The same techniques are used for solving Eqs. (3.2b) and (3.2c) for determining $T_{ijk}^{n+2/3}$ and T_{ijk}^{n+1}.

3.2.4. Truncation error and stability

The spatial accuracy of the spline approximation for interior points has been considered in the work of Rubin and Khosla [18].

For diffusion terms, the *cubic spline approximation* has second-order accuracy, which can be maintained even with rather large non-uniformities in mesh width.

For the linear heat conduction Eq. (3.1) with $Q=0$, the interior point stability of scheme (3.2) can be assessed with the Von Neumann Fourier decomposition for $\Delta x_{ijk}=\Delta y_{ijk}=\Delta z_{ijk}=h=$ constant.

Let

$$T_{ijk}^{n+1/3}=\bar{T}_{k_1k_2k_3}^{n+1/3}\,e^{I(k_1ih+k_2jh+k_3kh)}$$

$$T_{ijk}^{n+2/3}=\bar{T}_{k_1k_2k_3}^{n+2/3}\,e^{I(k_1ih+k_2jh+k_3kh)}$$

$$T_{ijk}^{n+1}=\bar{T}_{k_1k_2k_3}^{n+1}\,e^{I(k_1ih+k_2jh+k_3kh)}$$

$$T_{i\pm1,\,jk}^{n+1/3}=\bar{T}_{k_1k_2k_3}^{n+1/3}\,e^{I(k_1(i\pm1)h+k_2jh+k_3kh)}$$

$$T_{i,\,j\pm1,\,k}^{n+2/3}=\bar{T}_{k_1k_2k_3}^{n+2/3}\,e^{I(k_1ih+k_2(j\pm1)h+k_3kh)}$$

$$T_{ij,\,k\pm1}^{n+1}=\bar{T}_{k_1k_2k_3}^{n+1}\,e^{I(k_1ih+k_2jh+k_3(k\pm1)h)}$$

Let

$\xi_1=\dfrac{\bar{T}_{k_1k_2k_3}^{n+1/3}}{\bar{T}_{k_1k_2k_3}^{n}}$ amplification factor in x-direction

$\xi_2=\dfrac{\bar{T}_{k_1k_2k_3}^{n+2/3}}{\bar{T}_{k_1k_2k_3}^{n+1/3<}}$ amplification factor in y-direction

$\xi_3=\dfrac{\bar{T}_{k_1k_2k_3}^{n+1}}{\bar{T}_{k_1k_2k_3}^{n+2/3}}$ amplification factor in z-direction

$\xi=\dfrac{\bar{T}_{k_1k_2k_3}^{n+1}}{\bar{T}_{k_1k_2k_3}^{n}}$ global amplification factor, $I^2=-1$

From Eqs. (3.2a) and (3.3a), we find

$$\xi_1=\frac{1}{1+\dfrac{3\alpha(1-(\alpha_{i+1/2}\,e^{I(k_1h)}+\alpha_{i-1/2}\,e^{-I(k_1h)}))}{2+\cos\,k_1h}}$$

where

$$\alpha=\frac{\Delta t(K_{i+1/2}+K_{i-1/2})}{\rho C\cdot h^2}>0$$

$$\alpha_{i+1/2} = \frac{K_{i+1/2}}{K_{i+1/2} + K_{i-1/2}}$$

$$\alpha_{i-1/2} = \frac{K_{i-1/2}}{K_{i+1/2} + K_{i-1/2}}$$

In some manner ξ_2 and ξ_3 are calculated:

$$\xi_2 = \frac{1}{1 + \dfrac{3\alpha(1 - (\beta_{j+1/2}\, e^{I(k_2 h)} + \beta_{j-1/2}\, e^{-I(k_2 h)}))}{2 + \cos\ k_2 h}}$$

$$\xi_3 = \frac{1}{1 + \dfrac{3\alpha(1 - (\gamma_{k+1/2}\, e^{I(k_3 h)} + \gamma_{k-1/2}\, e^{-I(k_3 h)}))}{2 + \cos\ k_3 h}}$$

where

$$\beta = \frac{\Delta t(K_{j+1/2} + K_{j-1/2})}{\rho C \cdot h^2} > 0 \quad \text{and}$$

$$\gamma = \frac{\Delta t(K_{k+1/2} + K_{k-1/2})}{\rho C \cdot h^2} > 0$$

From $\xi = \xi_1 \cdot \xi_2 \cdot \xi_3$ we have $|\xi| \le |\xi_1| \cdot |\xi_2| \cdot |\xi_3|$.

ψ has to be bounded when t tends to 0, then $|\xi|$ have to be lower or equal to one.

The Von Neuman's condition for this scheme necessary for the suppression of all error growth requires that the spectral radius $|\xi| \le 1$.

With each of the coefficients, ξ_1, ξ_2 and ξ_3 less than one, their product is less than one and the scheme (3.2) is unconditionally stable with arbitrary values of Δt, h, K_i, K_j and K_k.

3.3. Computational algorithm

The heat transfer through the basement wall does not involve heat generation. By using Eq. (3.5), one can create the following system of linear equations:

$$AT = B$$

where A is an $(N \times N)$ matrix and T and B are (N) vectors. The subscript of A, T and B range from one to N as follows:

$$A = \begin{bmatrix} a_{1,1} & a_{1,2} & & & & \\ a_{2,1} & a_{2,2} & a_{2,3} & & & \\ & \cdots & \cdots & \cdots & & \\ & & \cdots & \cdots & \cdots & \\ & & & a_{n-1,n-2} & a_{n-1,n-1} & a_{n-1,n} \\ & & & & a_{n,n-1} & a_{n,n} \end{bmatrix}$$

$$T = \begin{pmatrix} T_1 \\ \cdots \\ \cdots \\ \cdots \\ \cdots \\ \cdots \\ T_n \end{pmatrix}, \quad B = \begin{pmatrix} D_1 - A_1 T_0 \\ D_2 \\ \cdots \\ \cdots \\ \cdots \\ D_{n-1} \\ D_n - C_n T_{n+1} \end{pmatrix}$$

where:

$$\begin{cases} a_{i+1,j} = A_i & \text{for } j = i \\ a_{i,j} = B_i & \text{for } j = i \\ a_{i,j} = C_i & \text{for } j = i+1 \\ a_{i,j} = 0 & \text{else} \end{cases}$$

The temperatures T_0 and T_{n+1} are the known s temperature.

The above system consists of a tri-diagonal of linear equations. To solve this system of equ the Thomas algorithm is used [22].

4. Results and discussions

While the complete review of results from the ment Consortium Research project is presentec where [3], the current paper elucidates and qua the effect of lateral heat flow with the help of th model.

4.1. Benchmarking of the model

This 3-D model is benchmarked with spatia temporal temperature distributions. In the initial lations, one forces the model to agree wit measured conditions by varying thermal condu of the material until finding the best fit. Ho there are hundreds of subsequent calculations in no further adjustment of material properties is al and where the model is used in a standard, pred manner.

Fig. 5 shows temperatures on both sides of t terior insulation (soil and concrete). The results o calculations on the test wall W6 during the s year are compared with the measured values. acceptable agreement between measured and calc temperature fields permits application of the mo quantify the effect of lateral heat flow.

4.2. Application of the model

As shown in Fig. 6, a reference calculation elim ing the lateral heat flow was called a 2-D solutio this case, the model calculations were perfo assuming that all materials properties are identic that of the EPS placed in the W5 position (i.e., terial on the side of the tested specimen). As sho

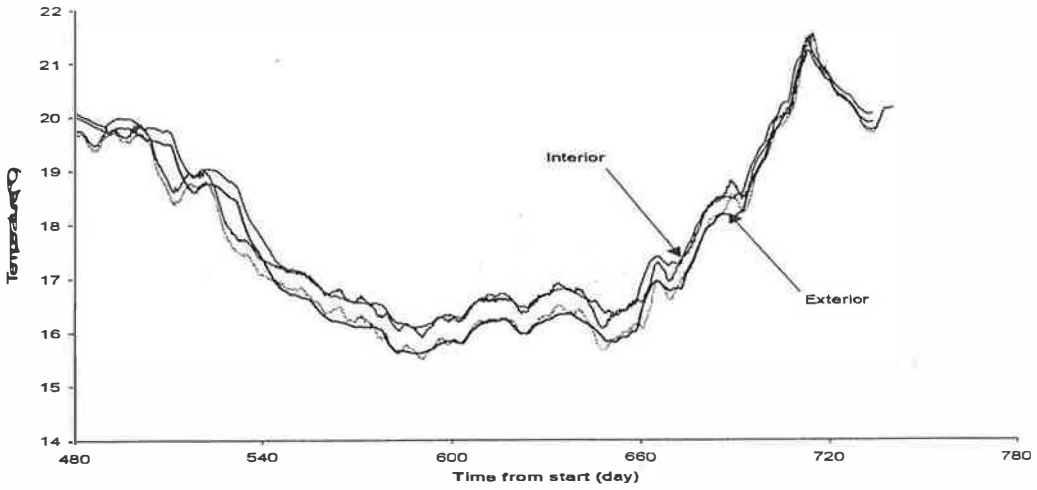

Fig. 5. Measured and simulated temperatures on both sides of the west wall, mid-height position.

Fig. 6, except for area adjacent to the corners, the temperature is uniformly distributed along the depth of the basement wall. In contrast to that uniformity, Fig. 7 shows the distribution of the temperature on the surface of the insulation, calculated for the actual temperature field, which was measured by thermocouples on the boundary of the control volume.

The model calculations, as previously discussed, were performed at three different positions where the heat flux incoming into the concrete wall was continually measured. Within these three locations the top position of the wall was the most sensitive to lateral heat flow. Fig. 8 shows the angle of the heat flux vector relative to the normal direction at the top position. It is evident that the thermal insulating system tested at the W6 position has a higher resistance to the heat flow than the adjacent materials W5 and W7. Moving from the centre towards the adjacent test specimen, one may observe that lines of heat flow start to deviate from the normal direction, reaching a maximum angle of about 10°. The lack of symmetry in Fig. 8 implies that the thermal resistance of EIBS in W5 differs from that in the W7 location. Also the performance of the corner guards W8 and W2 is different, although Fig. 8 shows that the width of these guards appear adequate to eliminate major disturbances from the adjacent test areas (W7 and W3).

Finally, Figs. 9a, 9b, 10a and 10b show the average relative thermal resistance of the specimen W6 when applying different models to the measured data (temperatures and heat fluxes) in the control volume during the first and second year of testing.

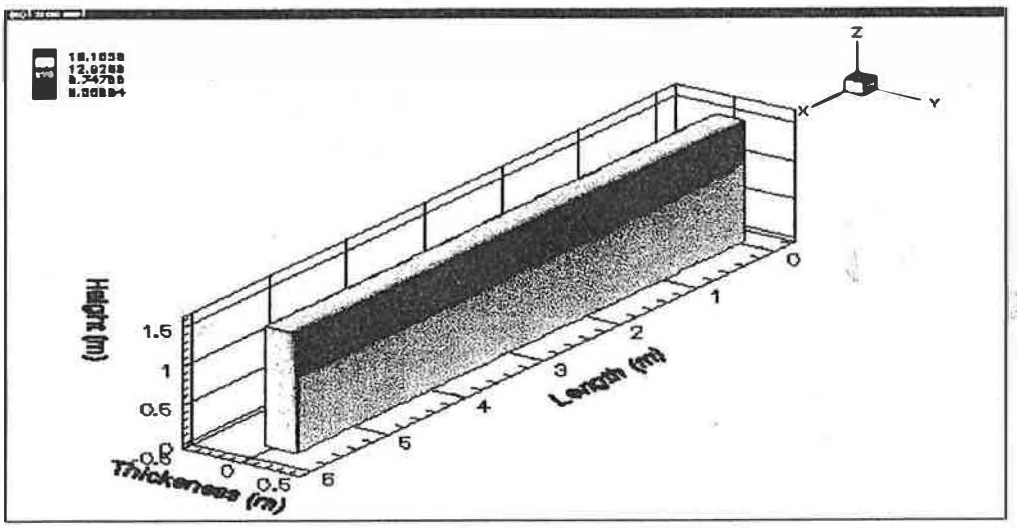

Fig. 6. Calculated temperatures on the soil–insulation interface of the west wall that would be there if all test specimens had properties equal to the W5 specimen (simulation). There is no lateral heat flow and therefore we call it a 2-D solution.

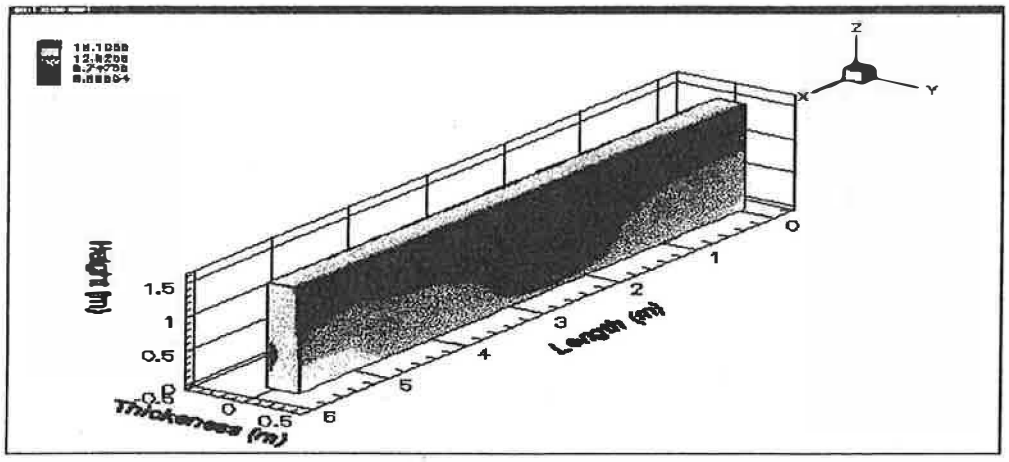

Fig. 7. The measured temperatures on the soil–insulation interface of the west wall.

The benchmark (100%) is the laboratory determined, initial value of thermal resistance of the specimen. The arbitrary nature of this benchmark will be discussed when discussing Part 3 of this research project, nevertheless it is sufficient for comparative purposes. Figs. 9a, 9b, 10a and 10b show such a comparison. Figs. 9a and b show results obtained with the 3-D analysis during the first and second year of testing, while Figs. 10a and b show the same calculations when the lateral heat flow component is eliminated (2-D model). These calculations are performed for the period during the second year of testing in which one-directional heat flow is prevailing (days 510–660).

Figs. 9a, 9b, 10a and 10b show that, in the worst case of the tested insulation systems, the yearly c ence between results obtained from 2- and 3-D m is about two percentage points for the first yea seven percentage points for the second year.

5. Concluding remarks

The Basement Consortium Research pr involved several different Exterior Basement Insul Systems placed next to each other. To evaluat effect of lateral heat flow in a concrete wall that as a heat sink or a source for adjacent specimens a different thermal resistance one needed a 3-D m

This model compared measured temperatures

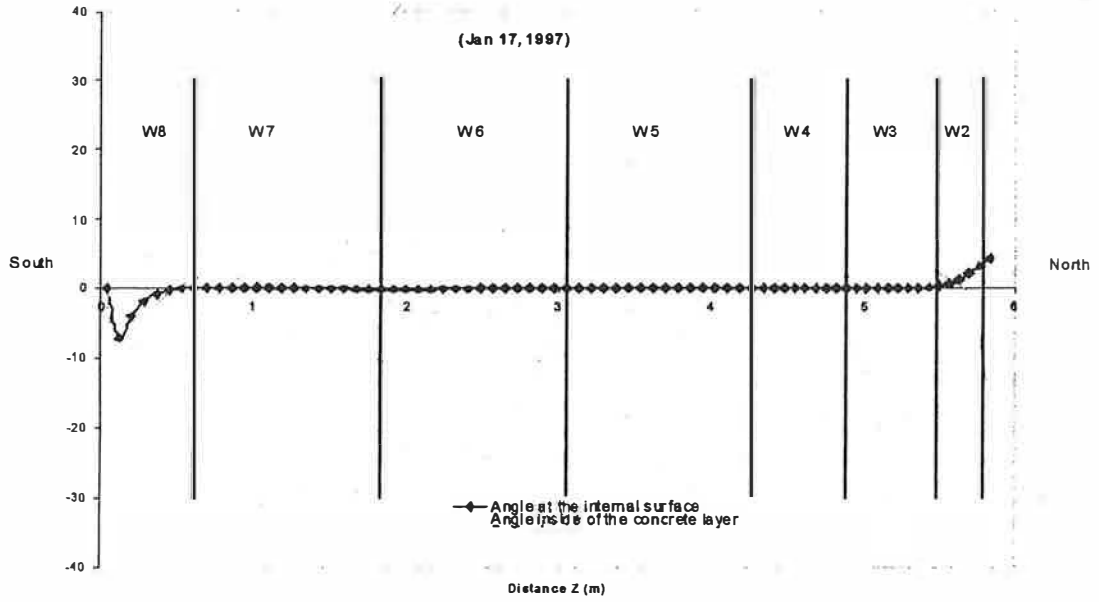

Fig. 8. Angle of the heat flux vector calculated at the top position of the west wall. Positive sign indicates the lateral flow in the southward tion.

heat fluxes in the test compartment with all tested compartments in the control element. The problem solver was based on the implicit Spline Method, which, for each computation step, stepwise reduces the 3-D conduction problem to a one tri-diagonal matrix of an implicit form solution.

Use of the 3-D model permitted a better assessment of the long-term thermal resistance of the thermal insulating systems used in the study. As shown in the above examples, the agreements between measured and calculated spatial and temporal temperature distributions are acceptable. Achieved in this manner, benchmarking of the model gives a degree of confidence in evaluating the effect of lateral heat flow. In the discussed example, the yearly difference between results obtained from 2- and 3-D models on the west wall was seven percentage points.

This analysis increased the confidence in estimating the effect of lateral heat flow significantly.

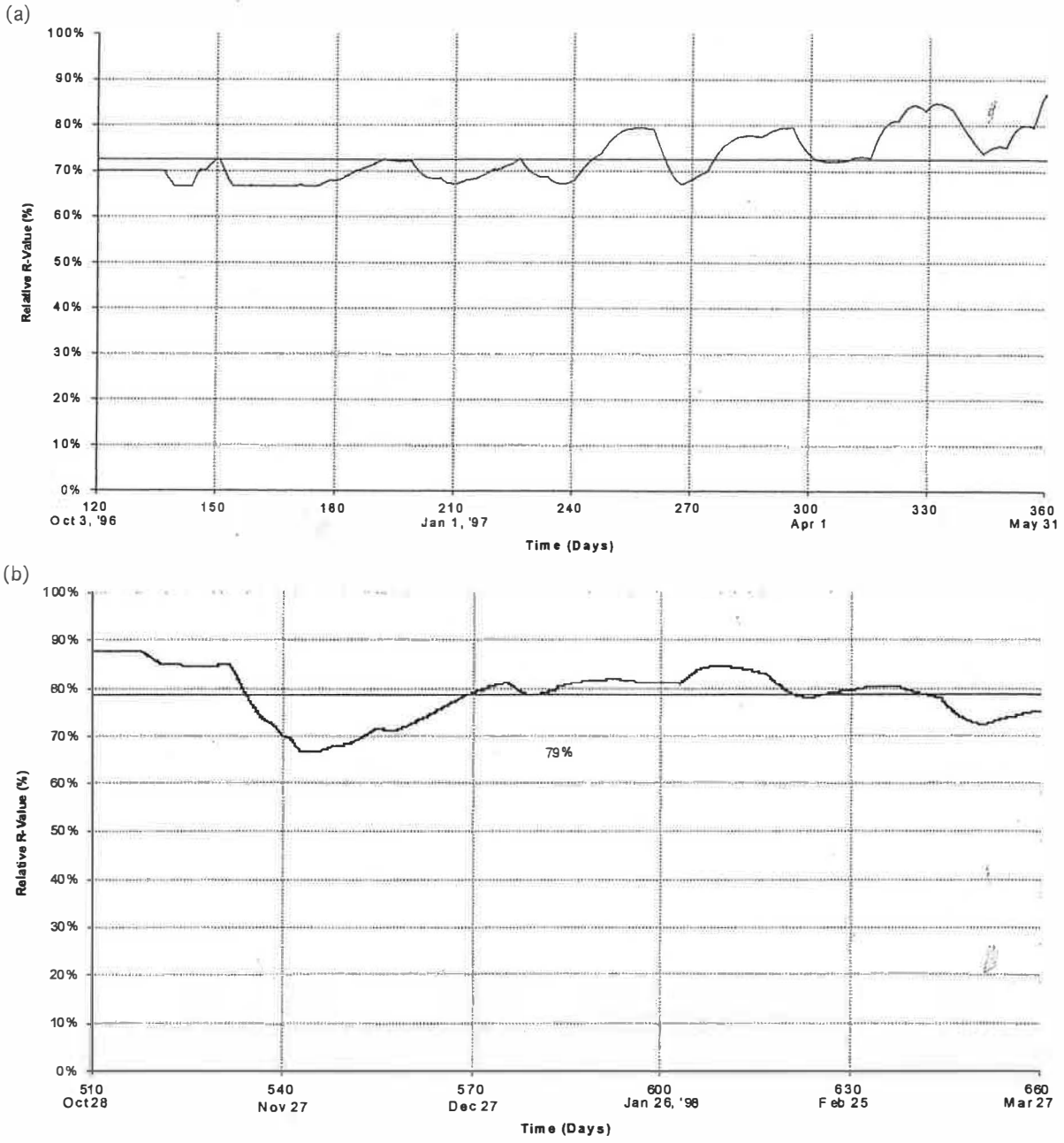

Fig. 9. Average relative thermal resistance of the specimen W-6 when applying the 3-D model to the measured data (temperatures and heat fluxes) in the control volume during (a) the first year of testing and (b) the second year of testing.

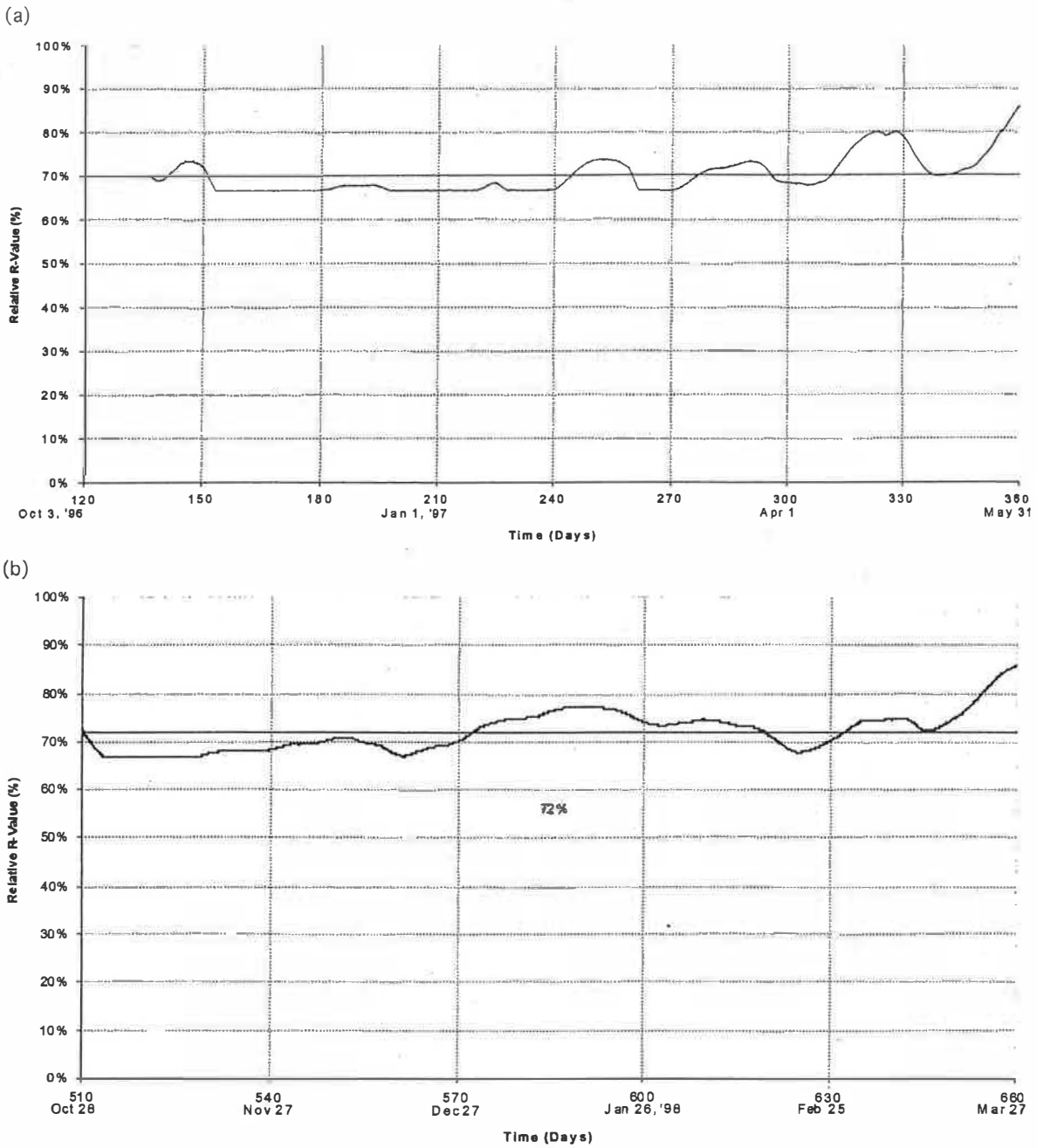

Fig. 10. Average relative thermal resistance of the specimen W-6 when applying the 2-D model to the measured data (temperatures an fluxes) in the control volume during (a) the first year of testing and (b) the second year of testing.

Acknowledgements

Deep gratitude and thanks are forwarded to Nicole Normandin who performed most of the experimental work, including data collection, and measured physical properties of tested specimens and to Roger Marchand who installed the data acquisition system and John Lackey who assisted Nicole Normandin in the experimental work.

References

[1] Tao SS, Bomberg MT, Hamilton JJ. Glass fiber as insu and drainage layer on exterior of basement walls. Symp on Thermal Insulation Performance, Tampa, FL, USA, ASTM Special Technical Publication, vol. 718 (NRCC-1 1980. pp. 57–76.

[2] Bomberg MT. Some performance aspects of glass fiber i tion on the outside of basement walls. Symposium on Th Insulation Performance, Tampa, FL, USA, 1978.

Special Technical Publications, vol. 718 (NRCC-19272), 1980. pp. 77–91.
[3] Swinton MC, Kumaran MK, Maref W, Bomberg MT. Performance of expanded polystyrene in the Exterior Insulation Basement Systems (EIBS). Journal of Thermal Envelope and Building Science 1999;23.
[4] Bomberg MT, Muzychka YS, Stevens DG, Kumaran MK. A comparative test method to determine thermal resistance under field conditions. J Thermal Insul and Bldg Envs 1994;18:163–82.
[5] Bhattacharya MC. An explicit conditionally stable finite difference equation for heat conduction problems. Int J Numer Methods Eng 1985;21:239–63.
[6] Lick W. Improved difference approximation to the heat equation. Int J Numer Methods Eng 1985;21:1957–69.
[7] Gurtin ME. Variational principles for linear initial-value problems. Q Appl Math 1964;22:252–6.
[8] Emery AF, Carson WW. An evaluation of the use of the finite element method in the computation of temperature. ASME J Heat Transfer 1971;39:136–45.
[9] Visser W. A finite element method for the determination of non-stationary temperature distribution and thermal deformations. In: Proceedings of the Conference on Matrix Methods in Structural Mechanics. Air Force Institute of Technology, Wright Patterson Air Force Base, Dayton, OH, 1965. p. 925–43.
[10] Bruch JC, Zyvolovski G. Transient two-dimensional heat conduction problems solved by the finite element method. Int J Numer Methods Eng 1974;8:481–94.
[11] Rources V, Alarcon E. Transient heat conduction problems using BIEM. Comput Struc 1983;16:717–30.
[12] Rizzo FJ, Shippy DJ. A method of solution for certain problems of transient heat conduction. AIAA J 1970;11:2004–9.
[13] Liggett JA, Liu PL-F. Unsteady flow in confined aquifers: a comparison of two boundary integral methods. Water Resour Res 1979;15:861–6.
[14] Cheng AH-D, Liggett JA. Boundary integral equation method for linear porous-elasticity with applications to soil consolidation. Int J Numer Methods Eng 1984;20:255–78.
[15] Chen H-K, Chen C-K. Application of hybrid Laplace transform/finite difference method to transient heat conduction problems. Numerical Heat Transfer 1988;14:343–56.
[16] Wang SP, Miao Y, Miao YM. An implicit spline method of splitting for the solution of multi-dimensional transient heat conduction problems. Proceedings of the Advanced Computational Methods in Heat Transfer, vol. 1, 1990. pp. 127–37.
[17] Rubin SG, Graves RA. Cubic Spline Approximation for Problems in Fluid Mechanics, NASA TR R-436 1975.
[18] Rubin SG, Khosla PK. Higher order numerical solutions using cubic splines. AIAA J 1976;14:851–8.
[19] Bomberg M, Kumaran K, Swinton M. On variability in physical properties of molded, expanded polystyrene. Journal of Thermal Envelope and Building Science 2000;23:244–65.
[20] Wang SP, Miao Y, Miao YM. An implicit spline method of splitting for the solution of multi-dimensional transient heat conduction problems. Proceedings of the first International Conference, Portsmouth, UK, 17–20 July 1990, 127–137.
[21] Maref W. Modelisation en Régime Dynamique du Comportement Thermique d'un Local Couplé à un plafond Rayonnant (Procédé Thermalu). Report of D.E.A. (September 1992), Pierre and Marie Curie University (Paris VI), 1992.
[22] Cranahan B, Luther HA, Wilkes JO. In: Applied numerical methods. New York: Wiley, 1969. p. 454–61.